J|A|C|S
ARTICLES
Published on Web 10/25/2006

Modulation of the Catalytic Behavior of α-Chymotrypsin at Monolayer-Protected Nanoparticle Surfaces

Chang-Cheng You, Sarit S. Agasti, Mrinmoy De, Michael J. Knapp, and Vincent M. Rotello*

Contribution from the Department of Chemistry, University of Massachusetts, 710 North Pleasant Street, Amherst, Massachusetts 01003

Received June 22, 2006; E-mail: rotello@chem.umass.edu

Abstract: Amino-acid-functionalized gold clusters modulate the catalytic behavior of α-chymotrypsin (ChT) toward cationic, neutral, and anionic substrates. Kinetic studies reveal that the substrate specificity (k_{cat}/K_M) of ChT−nanoparticle complexes increases by ∼3-fold for the cationic substrate but decreases by 95% for the anionic substrate as compared with that of free ChT, providing enhanced substrate selectivity. Concurrently, the catalytic constants (k_{cat}) of ChT show slight augmentation for the cationic substrate and significant attenuation for the anionic substrate in the presence of amino-acid-functionalized nanoparticles. The amino acid monolayer on the nanoparticle is proposed to control both the capture of substrate by the active site and release of product through electrostatic interactions, leading to the observed substrate specificities and catalytic constants.

Introduction

Modulation of enzyme activity provides a potent means to gain control over cellular processes such as signal transduction, DNA replication, and metabolism. On the other hand, aberrant activities of some enzymes can lead to the development of numerous diseases and disorders including cancers and human immunodeficiency virus (HIV) disease.[1,2] From this point of view, the modulation of enzyme activity is of great importance in therapeutics and pharmaceutics.[3] Synthetic small organic molecules (e.g., most drugs) have been used to inhibit the enzyme activity through the direct interaction with the active sites of enzymes.[4] Recent advances in nanoscale materials offer a new pathway for regulating enzyme behavior through surface interactions, providing a promising alternative to small molecule inhibition. Nanomaterials possess at least two attributes not possessed by small molecule ligands: First, they may provide large surface areas for efficient protein binding, as typically >6 nm^2 of buried surface are involved in forming protein−protein interfaces in nature.[5] Second, multivalent functionalities can be grafted on the materials to meet the structural complexity of proteins. Among diverse nanoscale entities, monolayer-protected nanoparticles are extremely attractive due to their ease of synthesis and structural diversity and have found successful applications in the interaction with proteins.[6,7]

As a representative serine protease, α-chymotrypsin (ChT) provides an excellent enzyme model for studying the modulation of activity due to its well-defined structure and extensively characterized enzymatic properties.[8] As illustrated in Figure 1a, the active pocket of ChT is surrounded by a ring of positively charged residues. Meanwhile, a number of hydrophobic "hot spots" are distributed on the surface. Such structural features allow the electrostatic interaction as well as hydrophobic interaction with receptors possessing complementary surfaces.

(1) (a) Harris, B. E.; Song, R.; Soong, S. J.; Diasio, R. B. *Cancer Res.* **1990**, *50*, 197−201. (b) Belinsky, S. A.; Nikula, K. J.; Baylin, S. B.; Issa, J.-P. J. *Proc. Natl. Acad. Sci. U.S.A.* **1996**, *93*, 4045−4050. (c) Burger, A. M.; Double, J. A.; Newell, D. R. *Eur. J. Cancer* **1997**, *33*, 638−644. (d) Armbruster, B. N.; Banik, S. S. R.; Guo, C. H.; Smith, A. C.; Counter C. M. *Mol. Cell. Biol.* **2001**, *21*, 7775−5586.

(2) (a) Shultz, M. D.; Ham, Y.-W.; Lee, S.-G.; Davis, D. A.; Brown, C.; Chmielewski, J. *J. Am. Chem. Soc.* **2004**, *126*, 9886−9887. (b) Overall, C. M.; Lopez-Otin, C. *Nat. Rev. Cancer* **2002**, *2*, 657−672. (c) Esler, W. P.; Wolfe, M. S. *Science* **2001**, *293*, 1449−1454. (d) Coussens, L. M.; Tinkle, C. L.; Hanahan, D.; Werb, Z. *Cell* **2000**, *103*, 481−490.

(3) (a) Leung, D.; Abbenante, G.; Fairlie, D. P. *J. Med. Chem.* **2000**, *43*, 305−341. (b) Aguiar, M.; Masse, R.; Gibbs, B. F. *Drug Metab. Rev.* **2005**, *37*, 379−404. (c) Miners, J. O.; Birkett, D. J. *Br. J. Clin. Pharmacol.* **1998**, *45*, 525−538.

(4) (a) Yin, F.; Cao, R.; Goddard, A.; Zhang, Y.; Oldfield, E. *J. Am. Chem. Soc.* **2006**, *128*, 3524−3525. (b) Demaegdt, H.; Laeremans, H.; De Backer, J.-P.; Mosselmans, S.; Le, M. T.; Kersemans, V.; Michotte, Y.; Vauquelin, G.; Vanderheyden, P. M. L. *Biochem. Pharmacol.* **2004**, *68*, 893−900. (c) Tan, Z.; Bruzik, K. S.; Shears, S. B. *J. Biol. Chem.* **1997**, *272*, 2285−2290. (d) Campbell, D. R.; Kurzer, M. S. *J. Steroid Biochem. Mol. Biol.* **1993**, *46*, 381−388. (e) Kozikowski, A. P.; Sun, H.; Brognard, J.; Dennis, P. A. *J. Am. Chem. Soc.* **2003**, *125*, 1144−1145. (f) Ding, K.; Lu, Y.; Nikolovska-Coleska, Z.; Qiu, S.; Ding, Y.; Gao, W.; Stuckey, J.; Krajewski, K.; Roller, P. P.; Tomita, Y.; Parrish, D. A.; Deschamps, J. R.; Wang, S. *J. Am. Chem. Soc.* **2005**, *127*, 10130−10131.

(5) Lo Conte, L.; Chothia, C.; Janin, J. *J. Mol. Biol.* **1999**, *285*, 2177−2198.

(6) (a) Niemeyer, C. M. *Angew. Chem., Int. Ed.* **2001**, *40*, 4128−4158. (b) Daniel, M.-C.; Astruc, D. *Chem. Rev.* **2004**, *104*, 293−346. (c) Katz, E.; Willner, I. *Angew. Chem., Int. Ed.* **2004**, *43*, 6042−6108. (d) Verma, A.; Rotello, V. M. *Chem. Commun.* **2005**, 303−312. (e) Gu, H.; Xu, K.; Xu, C.; Xu, B. *Chem. Commun.* **2006**, 941−949. (f) You, C.-C.; Verma, A.; Rotello, V. M. *Soft Matter* **2006**, *2*, 190−204.

(7) (a) Zheng, M.; Huang, X. *J. Am. Chem. Soc.* **2004**, *126*, 12047−12054. (b) Xu, C.; Xu, K.; Gu, H.; Zhong, X.; Guo, Z.; Zheng, R.; Zhang, X.; Xu, B. *J. Am. Chem. Soc.* **2004**, *126*, 3392−3393. (c) Abad, J. M.; Mertens, S. F. L.; Pita, M.; Fernandez, V. M.; Schriffrin, D. J. *J. Am. Chem. Soc.* **2005**, *127*, 5689−5694. (d) Aubin-Tam, M.-E.; Hamad-Schifferli, K. *Langmuir* **2005**, *21*, 12080−12084. (e) Kogan, M. J.; Bastus, N. G.; Amigo, R.; Grillo-Bosch, D.; Araya, E.; Turiel, A.; Labarta, A.; Giralt, E.; Puntes, V. F. *Nano Lett.* **2006**, *6*, 110−115. (f) Ackerson, C. J.; Jadzinsky, P. D.; Jensen, G. J.; Kornberg, R. D. *J. Am. Chem. Soc. 2006*, *128*, 2635−2640.

(8) (a) Blow, D. M. *Acc. Chem. Res.* **1976**, *9*, 145−152. (b) Cassidy, C. S.; Lin, J.; Frey, P. A. *Biochemistry* **1997**, *36*, 4576−4584.

10.1021/ja064433z CCC: $33.50

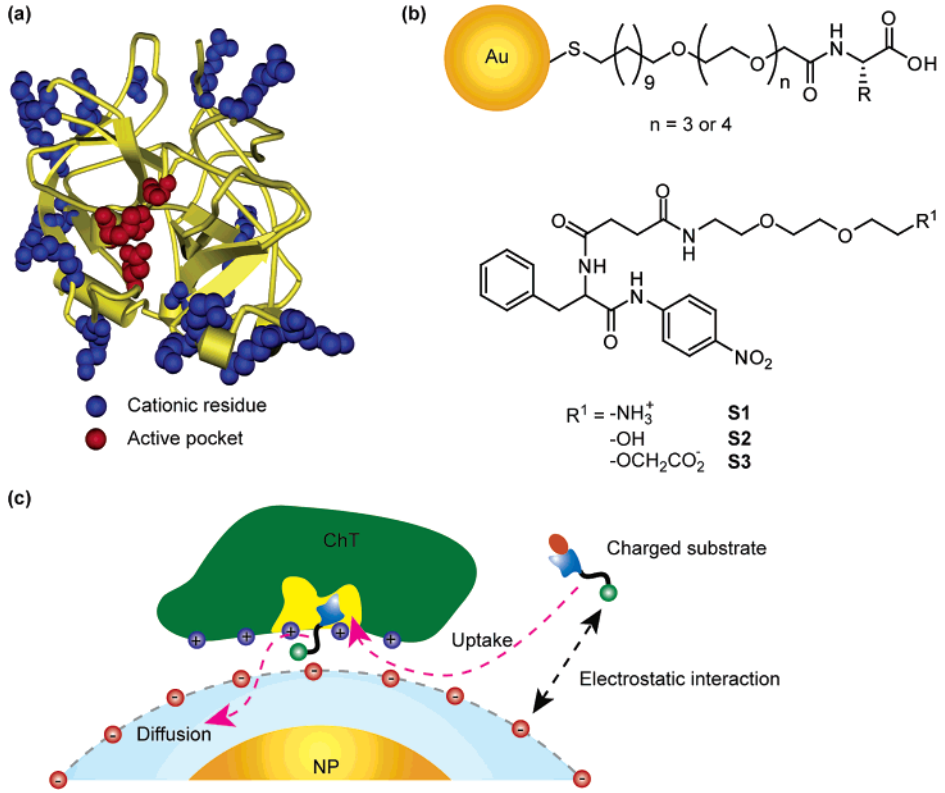

Figure 1. (a) Molecular structure of α-chymotrypsin. (b) Chemical structure of amino-acid-functionalized gold nanoparticles and SPNA-derived substrates. (c) Schematic representation of monolayer-controlled diffusion of the substrate into and the product away from the active pocket of nanoparticle-bound ChT.

Macrocyclic hosts[9] and surfactant micelles[10] have been used so far to improve the activity and stability of ChT in organic solvents through surface binding.

We have demonstrated that carboxylic-acid-functionalized nanoparticles can effectively associate with α-chymotrypsin through surface complementary charges to afford supramolecular complexes, resulting in the inhibition of its enzymatic activity toward anionic substrates such as *N*-succinyl-L-phenylalanine *p*-nitroanilide (SPNA).[11,12] This phenomenon has been attributed to the obstruction of the active site by the complex formation which reduces the accessibility of the substrates. Interestingly, in a follow-up study[13] we found that the association of ChT with the simple carboxylic acid monolayer-protected nanoparticles results in differential behavior with varying substrates. Nanoparticle-bound ChT showed no activity change toward the positively charged substrates, in contrast to the significant activity depression toward anionic substrates. In the current study, we systematically investigate the enzymatic kinetics of ChT in the presence of various amino-acid-functionalized gold nanoparticles (Figure 1b). The structural diversity of amino acids allows us to probe the role of various functional groups in controlling enzymatic function. With SPNA derivatives bearing positive, neutral, or negative end groups as substrates, we have demonstrated that the interaction between the nanoparticle monolayer and the substrates affects both k_{cat} and K_M values, resulting in an enhanced substrate selectivity for nanoparticle-bound ChT. Such results are ascribed to the monolayer-controlled uptake of the substrates and diffusion away of the products through electrostatic interactions (Figure 1c). In nature, electrostatic interactions play an important role in the uptake of substrates by many diffusion-controlled enzymes including superoxide dismutase (SOD),[14] acetylcholinesterase (AChE),[15] and triosephosphate isomerase (TIM).[16] The surface recognition of ChT by charged nanoparticles provides a means to mimic this strategy by tuning enzyme−substrate association.

Results and Discussion

Our previous study demonstrated that amino-acid-functionalized nanoparticles and ChT can form high affinity complexes in dilute sodium phosphate buffer (5 mM, pH 7.4).[12] To probe

(9) (a) Griebenow, K.; Laureano, Y. D.; Santos, A. M.; Clemente, I. M.; Rodriquez, L.; Vidal, M. W.; Barletta, G. *J. Am. Chem. Soc.* **1999**, *121*, 8157−8163. (b) Hasegawa, M.; Yamamoto, S.; Kobayashi, M.; Kise, H. *Enzyme Microb. Technol.* **2003**, *32*, 356−361. (c) Tremblay, M.; Cote, S.; Voyer, N. *Tetrahedron* **2005**, *61*, 6824−6828.

(10) (a) Spreti, N.; Profio, P. D.; Marte, L.; Bufali, S.; Brinchi, L.; Savelli, G. *Eur. J. Biochem.* **2001**, *268*, 6491−6497. (b) Abuin, E.; Lissi, E.; Duarte, R. *Langmuir* **2003**, *19*, 5374−5377. (c) Celej, M. S.; D'Anderea, M. G.; Campana, P. T.; Fidelio, G. D.; Bianconi, M. L. *Biochem. J.* **2004**, *378*, 1059−1066. (d) Abuin, E.; Lissi, E.; Duarte, R. *J. Colloid Interface Sci.* **2005**, *283*, 539−543.

(11) (a) Fischer, N. O.; McIntosh, C. M.; Simard, J. M.; Rotello, V. M. *Proc. Natl. Acad. Sci. U.S.A.* **2002**, *99*, 5018−5023. (b) Hong, R.; Fischer, N. O.; Verma, A.; Goodman, C. M.; Emrick, T.; Rotello, V. M. *J. Am. Chem. Soc.* **2004**, *126*, 739−743.

(12) (a) You, C.-C.; De, M.; Han, G.; Rotello, V. M. *J. Am. Chem. Soc.* **2005**, *127*, 12873−12881. (b) You, C.-C.; De, M.; Rotello, V. M. *Org. Lett.* **2005**, *7*, 5685−5688.

(13) Hong, R.; Emrick, T.; Rotello, V. M. *J. Am. Chem. Soc.* **2004**, *126*, 13572−13573.

(14) (a) Getzoff, E. D.; Tainer, J. A.; Weiner, P. K.; Kollman, P. A.; Richardson, J. S.; Richardson, D. C. *Nature (London)* **1983**, *306*, 287−290. (b) Allison, S. A.; Bacquet, R. J.; McCammon, J. A. *Biopolymers* **1988**, *27*, 251−269. (c) Davis, M. E.; Madura, J. D.; Sines, J.; Luty, B. A.; Allison, S. A.; McCammon, J. A. *Methods Enzymol.* **1991**, *202*, 473−497.

(15) (a) Quinn, D. M. *Chem. Rev.* **1987**, *87*, 955−979. (b) Tan, R. C.; Truong, T. N; McCammon, J. A.; Sussman, J. L. *Biochemistry* **1993**, *32*, 401−403.

(16) (a) Wade, R. C.; Gabdoulline, R. R.; Luty, B. A. *Proteins* **1998**, *31*, 406−416. (b) Jogl, G.; Rozovsky, S.; McDermott, A. E.; Tong, L. *Proc. Natl. Acad. Sci. U.S.A.* **2003**, *100*, 50−55.

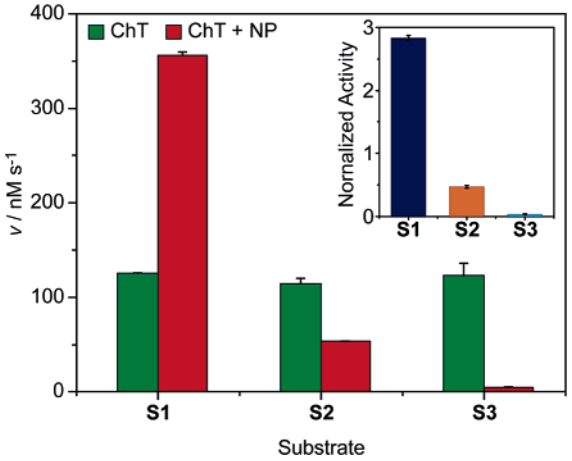

Figure 2. Generation rate (v) of 4-nitroaniline from different substrates (2.0 mM) under catalysis by ChT (3.2 μM) or ChT−**NP_4EG_Glu** complex (3.2 μM/0.8 μM). Inset shows the normalized activity of ChT−NP complex to ChT toward different substrates.

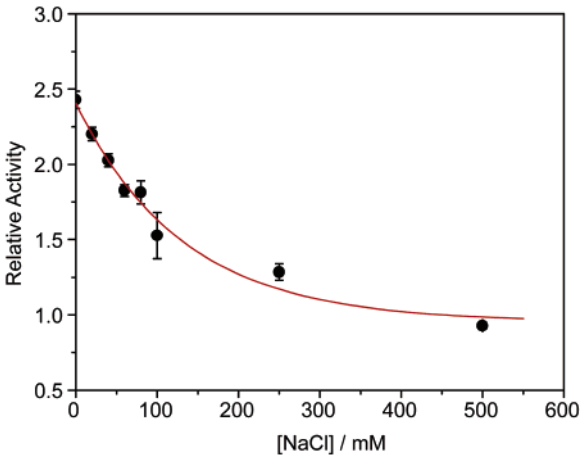

Figure 3. Relative activity of ChT−**NP_4EG_Glu** complex against **S1** at varying NaCl concentrations. The activities were normalized to that of free ChT at respective salt solutions. Line was added to guide eyes.

the effect of nanoparticles on ChT activity, a glutamic-acid-functionalized nanoparticle (**NP_4EG_Glu**,[17] 0.8 μM) was first incubated with ChT (3.2 μM) and the activity of the supramolecular complexes was investigated against different substrates in the same buffer system. As shown in Figure 2, native ChT has comparable activities toward the three substrates with diverse charge characteristics (**S1**−**S3**). Upon binding to **NP_4EG_Glu**, however, ChT shows distinctly different catalytic behaviors toward these substrates. For cationic substrate **S1**, ChT activity increases by ca. 3-fold. For neutral and negatively charged substrates **S2** and **S3**, however, ChT activity decreases by ca. 50% and ca. 95%, respectively. These observations demonstrated that nanoparticle receptors can tune, rather than simply inhibit, the activity of ChT.

Activity assays were performed at varying salt concentrations to verify that the changes of enzymatic activity arise from the formation of protein−particle complexes. In the control experiments, slightly enhanced activity was observed for free ChT with increasing salt concentrations (ca. 30% in 500 mM NaCl). Therefore, the activity of the ChT−nanoparticle couple was normalized to that of free ChT at the same salt concentrations to eliminate this effect. As shown in Figure 3, the normalized activity of ChT−**NP_4EG_Glu** toward substrate **S1** decreases with increasing salt concentrations and reaches a plateau in NaCl solutions of above 500 mM. We have demonstrated that the driving force for the ChT−nanoparticle complex formation is surface complementary electrostatic interaction. The presence of a large amount of competitive ions would attenuate such interaction.[18] In this context, the observed phenomenon indicates that the superactivity of ChT−**NP_4EG_Glu** toward **S1** is related to complex formation. The intrinsic activity of ChT recovered along with the collapse of the complexes at elevated salt concentrations. Similarly, the activity of ChT−**NP_4EG_Glu** toward anionic substrate **S3** increases with the increase of salt concentration in a sigmoidal profile, which is also attributed to the complex disruption at higher salt concentrations.

Kinetic data for ChT activity are crucial for understanding its enzymatic behavior in the presence of amino-acid-functionalized nanoparticles. It has been well demonstrated that α-chymotrypsin-catalyzed hydrolysis of amide substrates is fully described by the three-step model shown in eq 1.[19] First, the enzyme reversibly binds substrate to give the enzyme−substrate complex (ES), followed by nucleophilic attack by the active site serine to form the acyl enzyme (ES′) intermediate and release the amine product (P_1). The amine product for all substrates used in this study is 4-nitroaniline. Hydrolysis of the acyl intermediate affords the free enzyme and the carboxylic acid (P_2) which retains the functional group (R^1) from the substrate.

$$\mathrm{E} + \mathrm{S} \underset{k_{-1}}{\overset{k_1}{\rightleftharpoons}} \mathrm{ES} \xrightarrow{k_2} \underset{+\ \mathrm{P_1}}{\mathrm{ES'}} \xrightarrow{k_3} \mathrm{E} + \mathrm{P_2} \qquad (1)$$

Applying the steady-state assumption to [ES′], the kinetics of the hydrolysis reaction can be analyzed in terms of eq 1 to give an identical form with the Michaelis−Menten equation. The general equations for velocity (v_0) and catalytic constants (k_{cat}) and substrate specificity constants (k_{cat}/K_M) are shown below:

$$v_0 = \frac{k_{cat}[\mathrm{E}][\mathrm{S}]}{K_M + [\mathrm{S}]} \qquad (2)$$

$$k_{cat} = \frac{k_2 k_3}{k_2 + k_3} \qquad (3)$$

$$k_{cat}/K_M = \frac{k_1 k_2}{k_{-1} + k_2} \qquad (4)$$

The activity of ChT in the absence and presence of various amino-acid-functionalized nanoparticles was investigated with varying substrate concentrations to quantify the Michaelis−Menten parameters. The formation of 4-nitroaniline was linearly

(17) The nanoparticle nomenclature initiates with NP followed by the number of ethylene glycol units and the three letter code of terminal amino acids. That is, **NP_4EG_Glu** represents glutamic-acid-functionalized gold nanoparticle with a tetra(ethylene glycol) tether.

(18) (a) Israelachvili, J. N. *Intermolecular and Surface Forces*, 2nd ed.; Academic Press: London, 1992. (b) Verma, A.; Simard, J. M.; Rotello, V. M. *Langmuir* **2004**, *20*, 4178−4181.

(19) Hedstrom, L. *Chem. Rev.* **2002**, *102*, 4501−4523.

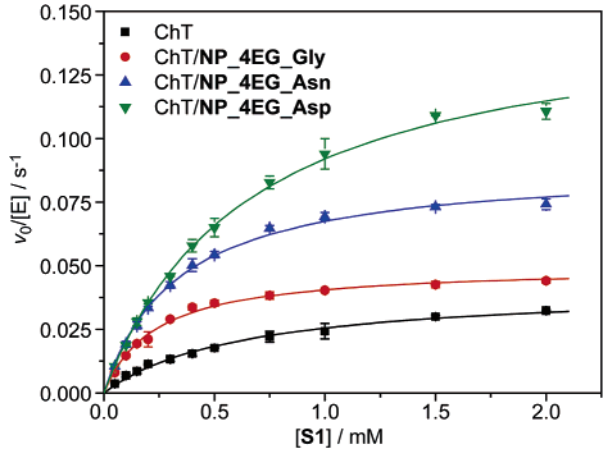

Figure 4. Substrate saturation curves for the hydrolysis of substrate **S1** by ChT (1.8 μM) in the absence and presence of various amino-acid-functionalized nanoparticles (0.45 μM) in sodium phosphate buffer (5 mM, pH 7.4) at 30 °C. The lines represent the best fit of the data using the Michaelis−Menten equation.

dependent on the reaction time during the monitoring period (15 min) at all the substrate concentrations used. The initial reaction rate (v_0) was thus calculated from the slope of absorption changes vs the reaction time, where the absorbance was converted to a concentration scale by a molar absorption coefficient of 9800 M^{-1} cm^{-1} for 4-nitroaniline.[20] Typical substrate saturation curves for the hydrolysis of **S1** by ChT and ChT−nanoparticle complexes are depicted in Figure 4. The solid lines represent the best fit of the data using eq 2.

From Figure 4, it is seen that the hydrolysis of the substrate **S1** by ChT and ChT−nanoparticle complexes follows the Michaelis−Menten mechanism. Interestingly, the substrate saturation curves are dependent on the structure of nanoparticle side chains. According to the binding constants and stoichiometries obtained previously,[12] it is estimated that >90% ChT molecules are bound to the nanoparticles to afford supramolecular complexes (refer also to Figure S1 in the Supporting Information) at the concentrations used, i.e., 1.8 μM ChT and 0.45 μM nanoparticles. Therefore, the differences on the Michaelis−Menten curves are attributed to the complex formation. Similar phenomena are also observed for the hydrolysis of substrates **S2** and **S3**. The kinetic parameters k_{cat}, K_M, and k_{cat}/K_M were subsequently evaluated from the nonlinear least-squares curve-fitting analysis using the Origin 7.0 program (OriginLab Co., Northampton, USA), which are compiled in Table 1.

It is noted from Table 1 that native ChT affords similar specificity constants (k_{cat}/K_M) for the charged **S1** and **S3** and a slightly smaller specificity constant for neutral **S2**. Upon binding to the amino-acid-functionalized nanoparticles, the specificity constants of ChT increase significantly for cationic **S1** but decrease for **S2** and **S3**. We attribute this to electrostatic interactions between the functionalized nanoparticles and substrates that affect substrate association with ChT. When acylation is much slower than substrate release ($k_{-1} \gg k_2$), then $k_{cat}/K_M = k_2/K_S$, where K_S denotes the dissociation constant of the ES complex. As nanoparticles bind to the surface of

(20) Sträter, N.; Sun, L.; Kantrowitz, E. R.; Lipscomb, W. N. *Proc. Natl. Acad. Sci. U.S.A.* **1999**, *96*, 11151−11155.

Table 1. Effect of Amino-Acid-Functionalized Gold Nanoparticles on Kinetic Parameters of α-Chymotrypsin[a]

substrate	enzyme	$k_{cat}/10^{-2}$ s^{-1}	K_M/mM	$k_{cat}/K_M/M^{-1}$ s^{-1}
	ChT	4.37	0.65	67.2
	ChT/**NP_4EG_Gly**	5.08	0.24	211.7
	ChT/**NP_4EG_Ala**	5.63	0.19	296.3
	ChT/**NP_4EG_Leu**	5.31	0.24	221.3
	ChT/**NP_4EG_Asp**	16.34	0.74	220.8
	ChT/**NP_4EG_Asn**	9.32	0.36	258.9
S1	ChT/**NP_4EG_Glu**	9.93	0.37	268.4
	ChT/**NP_4EG_Gln**	5.85	0.22	265.9
	ChT/**NP_3EG_Gly**	6.70	0.24	279.2
	ChT/**NP_3EG_Leu**	6.35	0.26	244.2
	ChT/**NP_3EG_Asp**	16.18	0.63	256.8
	ChT/**NP_3EG_Asn**	9.29	0.35	265.4
	ChT/**NP_3EG_Glu**	10.74	0.43	249.8
	ChT/**NP_3EG_Gln**	8.16	0.26	313.8
	ChT	5.40	1.5	36.0
S2	ChT/**NP_4EG_Leu**	6.46	6.6	9.8
	ChT/**NP_4EG_Asp**	5.46	3.5	15.6
	ChT/**NP_4EG_Glu**	5.40	3.9	13.8
	ChT	6.18	0.83	74.5
S3	ChT/**NP_4EG_Leu**	0.26	2.0	1.3
	ChT/**NP_4EG_Asp**	0.29	1.1	2.6
	ChT/**NP_4EG_Glu**	0.26	1.2	2.1

[a] Sodium phosphate buffer solution (5 mM, pH 7.4) at 30.0 °C. [ChT] = 1.8 μM, [NP] = 0.45 μM. The experimental errors are within 10%.

ChT and the acylation step is largely confined within the active site, ChT binding to nanoparticles is more likely to alter the dissociation constant for substrate (K_S) than to affect acylation, k_2. For cationic substrate **S1**, k_{cat}/K_M increases ~4-fold upon ChT binding to the anionic particles, suggesting that K_S has decreased. Similarly, the decrease of k_{cat}/K_M for **S2** and **S3** is attributed to an increasing K_S for nanoparticle-bound ChT.

Although k_{cat}/K_M is generally regarded as the "specificity constant" or "catalytic proficiency", this value is actually disconnected from real rates of net product formation and complete catalytic turnovers. Northrop has suggested that k_{cat}/K_M can be viewed as the ability of an enzyme to capture its substrates.[21] As the substrates differ from each other only by their charge, it seems that the ability of ChT−nanoparticle complexes to capture these substrates is highly dependent upon substrate charge. To understand this phenomenon, the pertinent structural features of the ChT−nanoparticle complexes need to be discussed. The nanoparticles associate with ChT through surface binding, while the active pocket of the enzyme is kept vacant, allowing the access of suitable substrates. Potential obstacles to substrate capture are steric hindrance and electrostatic interactions with the anionic monolayer of nanoparticles near the entrance of the active site (Figure 5a). The electrostatic attraction between the cationic substrate **S1** and the anionic monolayer facilitates the accumulation of this substrate at the nanoparticle surface, increasing its local concentration. The favorable electrostatic attraction results in the facilitated substrate capture. For neutral substrate **S2**, there is only a moderate reduction in substrate capture as there is merely steric hindrance present. When the anionic substrate **S3** is employed, the electrostatic repulsion between the monolayer and substrate further reduces the accessibility of the substrate to the enzyme, leading to the poorest capture. Thus, our results are entirely

(21) Northrop, D. B. *J. Chem. Edu.* **1998**, *75*, 1153−1157.

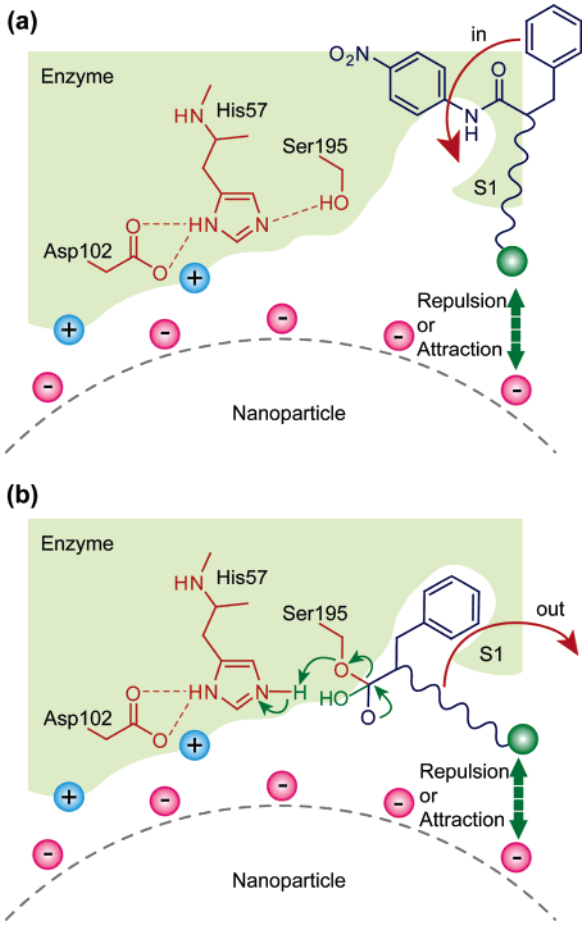

Figure 5. Electrostatic interaction-controlled (a) uptake of the substrate and (b) removal of the carboxylate product within the nanoparticle-bound enzyme.

consistent with the monolayer of nanoparticle acting as a selectivity filter which either enhances or diminishes substrate access to the active site.

Electrostatic interactions play a key role in biomacromolecular binding, an effect that is mimicked in forming the ChT−nanoparticle complexes. Small-molecule steering by electrostatics is also found in many enzymes, such that charged substrates bind to the active sites with enhanced affinity. In Cu/Zn SOD the local positive charge provided by Lys and Arg residues steers the anionic substrate, $O_2^{-\bullet}$, toward the active site.[14a] This leads to a remarkably high rate of turnover ($k_{cat}/K_M \sim 10^9$ M^{-1} s^{-1}) that is partially limited by diffusion. A similar situation is found in human H-chain ferritin, where electrostatic gradients found at channels are suggested to guide cations, such as aquated Fe^{3+}, entering or leaving the mineralized ferric hydroxide core.[22] Acetylcholinesterase has a highly anionic pore leading to the active site, which engenders rapid turnover of the cationic substrate acetylcholine.[15] The ChT−nanoparticle adducts gain a similar selectivity filter by virtue of the charged monolayer from the nanoparticle.

Although the free ChT shows comparable specificity for three substrates (**S1**−**S3**), the k_{cat}/K_M values for ChT complexed with a given nanoparticle always decrease in the order **S1** > **S2** > **S3** (Table 1). For example, ChT shows a selectivity of 0.9 for **S1** relative to **S3**, but this value is increased by 140-fold to ca. 125 once ChT is bound to glutamic-acid-functionalized nanoparticles. When a leucine-functionalized nanoparticle is employed, an even higher substrate selectivity of 170 for the **S1** and **S3** couple is obtained. It is necessary to point out that the k_{cat}/K_M values vary only in a small range for a certain substrate against different ChT−nanoparticle systems due to the compensation effect between k_{cat} and K_M (vide post). Nevertheless, such results demonstrate that monolayer-controlled uptake of substrates provides a powerful means for enhancing the substrate selectivity of enzymes.

From Table 1, it is also interesting to note that the catalytic constant (k_{cat}) of ChT when complexed with nanoparticles is again related to the charge of substrates. That is, ChT displays a slight increase in k_{cat} for cationic substrate **S1**, essentially no change for neutral substrate **S2**, and drastically decreases for anionic substrate **S3** in the presence of nanoparticles. As the local pH for both anionic and cationic substrates in the presence of a certain nanoparticle should be similar, the observed variation of k_{cat} values cannot originate from the local pH changes. Since the catalytic constant is related to the formation (k_2) and decomposition (k_3) of the acyl intermediate, nanoparticles could affect either process. Bender and co-workers have proposed that acylation is a rate-limiting step for the hydrolysis of amide substrates while deacylation is rate-determining for the hydrolysis of ester substrates of serine proteases, a mechanism that has gained wide acceptance.[23] However, some experiments suggest that, even in the case of amides, deacylation can be a rate-limiting step.[24]

In the current case, we propose that k_{cat} is determined by product release, a step which is combined with deacylation into k_3. Three separate arguments support this proposal. First, if ChT−NP binding does not perturb the active site, then acylation (k_2) will be little affected by the presence of the nanoparticles; any changes in k_{cat} must result from changes in k_3. Second, k_{cat} and k_{cat}/K_M vary independently for most of the nanoparticles in Table 1, indicating that the rate-limiting step for k_{cat} is not found in the expression for k_{cat}/K_M; this excludes k_2 as the rate-limiting step on k_{cat} for all but the fastest ChT−nanoparticle adducts. Third, a "burst phase" is always observed for the ChT-catalyzed hydrolysis of the substrates before the reaction levels off to a slower steady-state rate (Figures S2 and S3 in the Supporting Information). As turnover was monitored by the release of 4-nitroaniline, such a phenomenon indicates that k_3 is the rate-determining step for the hydrolysis reaction.[25] Therefore, the observed changes of k_{cat} values are mainly attributed to the effect of nanoparticles on the release of P_2. As shown in Figure 5b, the deacylation process involves not only hydrolysis of the acyl enzyme but also the diffusion of the second product (P_2) from the active site to regenerate free enzyme. The diffusion process should be related to the electrostatic interactions between the charged substrates and the anionic monolayer of the nanoparticles, mirroring the effect seen for substrate binding. For the cationic substrates, as P_2 contains the positively charged tail, release from the active site appears to be facilitated by the

(22) Douglas, T.; Ripoll, D. R. *Protein Sci.* **1998**, *7*, 1083−1091.

(23) (a) Zerner, B.; Bond, R. P. M.; Bender, M. L. *J. Am. Chem. Soc.* **1964**, *86*, 3674−3679. (b) Bender, M. L.; Kezdy, F. J.; Gunter, C. R. *J. Am. Chem. Soc.* **1964**, *86*, 3714−3721.

(24) (a) Christenen, U.; Ipsen, H.-H. *Biochim. Biophys. Acta* **1979**, *569*, 177−183. (b) Stein, R. L.; Viscarello, B. R.; Wildonger, R. A. *J. Am. Chem. Soc.* **1984**, *106*, 796−798. (c) Wang, E. C. W.; Hung, S.-H.; Cahoon, M.; Hedstrom, L. *Protein Eng.* **1997**, *10*, 405−411.

(25) Hartley, B. S.; Kilby, B. A. *Biochem. J.* **1954**, *56*, 288−297.

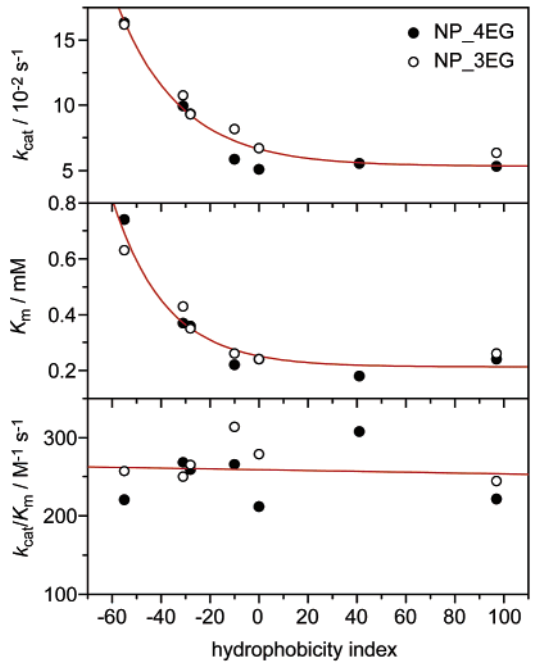

Figure 6. Correlation of kinetic parameters of ChT/NP complexes against substrate **S1** to the hydrophobicity index of amino acid side chain in nanoparticles. Lines were added to guide the eye.

electrostatic attraction to the negatively charged nanoparticles. By contrast, the negatively charged P_2 resulting from anionic **S3** experiences electrostatic repulsion with the anionic monolayer, leading to a reduced rate of product release. Consequently, the observed k_{cat} value for cationic substrates increases whereas the value for anionic substrates decreases in the presence of nanoparticles. For the neutral substrate **S2**, the deacylation process is not affected by the presence of nanoparticles due to the absence of charged functionalities. Essentially the same k_{cat} values are observed for this substrate before and after complexation of ChT with nanoparticles.

For substrates **S2** and **S3**, the catalytic constants of ChT−nanoparticle do not change significantly with respect to the amino acid functionalities. However, the systematic investigation on the hydrolysis of **S1** by ChT in the presence of various nanoparticles revealed that the catalytic behavior is dependent on the properties of the amino acid side chains. We have demonstrated previously that the hydrophobicity of amino acid side chains can affect the binding strength between the nanoparticles and the protein.[12] Herein, we plot the enzyme kinetic constants against the hydrophobicity index[26] of amino acid side chains in the nanoparticles. As can be seen from Figure 6, the k_{cat} and K_M values decrease smoothly according to the hydrophobicity index, whereas k_{cat}/K_M is nearly invariant. For cationic substrate **S1**, the different nanoparticle−ChT complexes afford essentially the same k_{cat}/K_M value of 258 ± 29 M^{-1} s^{-1}, irrespective of the hydrophobicity index. If we view k_{cat}/K_M as the ability of the enzyme−particle complexes to capture the substrate, then nanoparticle functionality does not impart selectivity in the uptake of the anionic **S1** by the enzyme bound to the nanoparticle surface. This result is reasonable as the redundant surface carboxylates of the nanoparticles can assist in the accumulation of cationic substrates on the nanoparticle surface and subsequently the uptake by the enzyme.

The sensitivity of k_{cat} to functionality, however, indicates that a step unique to k_{cat} depends on the surface functionality. The only such step in the kinetic scheme (eq 1) is the release of P_2 (k_3). The release of the cationic P_2 is enhanced by the more hydrophilic groups. We can see that the k_{cat} values decrease as the amino acid side chains become more hydrophobic, irrespective with the length of the oligo(ethylene glycol) tethers. Although the k_{cat} values seem to correlate with hydrophobicity, this may mask the real correlation. From Table 1, we can note that complexes of ChT with nanoparticles functionalized with dianionic amino acids such as aspartic acid and glutamic acid always give the highest catalytic constants. As we have discussed above, the electrostatic interaction controls the release of the hydrolyzed product away from the active site. If there are more negative charges on the monolayer, the electrostatic attraction would increase P_2 release within the charged microenvironment. Consequently, it is not surprising to see that the nanoparticles with dianionic amino acids show the highest k_{cat} values. In this context, the correlation between k_{cat} values and hydrophobicity indices indeed reflects the correlation of k_{cat} with the charge of the side chain, as the more charge the side chain has, the more hydrophilic it is.

Conclusion

In summary, we have systematically investigated the enzymatic kinetics of ChT upon binding to amino-acid-functionalized gold nanoparticles toward different substrates and demonstrated that the complex formation provides a powerful tool to tune the enzyme specificity. The association of ChT with anionic nanoparticles leads to the increase of specificity to the positively charged substrate and the decrease of specificity to the negatively charged substrate. Such enhanced substrate selectivity originates from the electrostatic interaction as well as the steric repulsion of the substrates with the nanoparticle monolayer. Significantly, the presence of nanoparticles can also affect the catalytic constants of the enzyme toward different substrates. The underlying mechanism is attributed to the electrostatic-interaction-controlled diffusion of the hydrolyzed product. These results revealed that the inhibition of the enzymes by nanoparticles is far different from that of conventional competitive or noncompetitive mechanisms. Monolayer-functionalized nanoparticles provide a potent scaffold for creation of an enzyme modulator based on surface recognition.

Experimental Section

Materials. α-Chymotrypsin (Type I−S from bovine pancreas) and *N*-succinyl-L-phenylalaine *p*-nitroanilide (SPNA) were purchased from Sigma and used as received. All the other chemicals were obtained from Aldrich or Fisher unless otherwise stated. Amino-acid-functionalized gold nanoparticles[12] and SPNA derivatives **S1**−**S3**[13] were synthesized according to the reported procedures. Disodium hydrogen and sodium dihydrogen phosphate were dissolved in deionized, distilled water (18 MΩ) to make a 5 mM phosphate buffer solution of pH 7.4, which was used throughout the enzymatic study.

Activity Assays. Activity assays were performed in sodium phosphate buffer (5 mM, pH 7.4) with [ChT] = 1.8 μM and [NP] = 0.45 μM and varied substrate concentrations (i.e., 0.05, 0.1, 0.15, 0.2, 0.3, 0.4, 0.5, 0.75, 1.0, 1.5, and 2.0 mM). The enzymatic hydrolysis reaction was initiated by adding a substrate stock solution (20 μL) in

(26) Monera, O. D.; Sereda, T. J.; Zhou, N. E.; Kay, C. M.; Hodges, R. S. *J. Pept. Sci.* **1995**, *1*, 319−329.

ethanol to a ChT−NP solution (180 μL). After pre-equilibrium for 3 min, enzyme activity was followed by monitoring product formation every 15 s for 15 min at 405 nm with a microplate reader (EL808IU, Bio-Tek Instruments, or SpectraMax M5, Molecular Devices). The assays were done in duplicate or triplicate, and the averages are reported. The absorbance was converted to a concentration scale by a molar extinction coefficient of 9800 M^{-1} cm^{-1} for 4-nitroaniline.[20] In the experiments of varying salt concentration, sodium chloride was added into the phosphate buffer (5 mM, pH 7.4) to make the corresponding solution.

Acknowledgment. This research was supported by the NSF Center for Hierarchical manufacturing at the University of Massachusetts (NSEC, DMI-0531171) and the ONR (N000140510501).

Supporting Information Available: Three figures (Figures S1−S3) for activity assays. This material is available free of charge via the Internet at http://pubs.acs.org

JA064433Z